HEAT TRANSFER IN STAR SHAPED POLYGONS

Fernando de Souza Costa
Laboratório Associado de Combustão e Propulsão, Instituto Nacional de Pesquisas Espaciais
Rodovia Presidente Dutra, km 40, Cachoeira Paulista, 12630-000, SP
fernando@lcp.inpe.br

Abstract. Monte Carlo methods have been used in a number of applications, including heat transfer, electromagnetics and neutron diffusion. This paper describes the application of the exodus method, a Monte Carlo method variation, to solve the Laplace equation. Probability matrices are generated by the exodus method, stored and then used to determine the full solutions inside squares and circles. Then, the Schwarz-Christoffel conformal mapping on the unit circle is applied to determine the temperature fields within m-pointed star shaped polygons with different boundary conditions.

Keywords: Exodus method, temperature distribution, probability matrix, Schwarz-Christoffel mapping, m-pointed star

1. INTRODUCTION

Emery and Carson (1968) developed initially the exodus method as a variation of the fixed random walk Monte Carlo method. Both methods are based on the displacement of particles throughout the grid formed by finite difference discretization of partial differential equations, such as the Laplace and Poisson equations. However, the exodus method, contrarily to the fixed random walk Monte Carlo method, does not require the generation of random numbers to determine the dispatch of particles within the computacional grid and, therefore, presents better computational efficiency.

Monte Carlo methods have been successfully used to solve electromagnetism, neutron diffusion and conduction heat transfer problems, considering different coordinate systems. Haji-Sheikh and Sparrow (1967) developed a floating random walk method to solve heat conduction problems. Fraley et al. (1980) used a new approach of the Monte Carlo method to solve heat conduction problems adopting a transport equation approximation. A variety of problems was analyzed with this method and their solutions were compared to those obtained with analytical techniques. Naraghi and Tsai (1993) presented a boundary-dispatch Monte Carlo method, in which the particles were dispatched from the boundaries of a conductive medium or source of heat. Particles of 2 or multiple species were dispatched from a boundary node and made random walks within the medium. Momoh et al. (2010) used the exodus method to solve the axisymmetric potential problem in spherical coordinates and computed the potential distribution in a conducting spherical shell.

In these applications, the Monte Carlo approach was limited to simple geometries and to the calculation of properties in a few points using course grids, mainly due to limitations in computational speed and data storage. Therefore, this paper applies the standard exodus method (EM) to generate probability matrices which are stored and used to solve heat conduction problems in a solid body with various boundary conditions. The full temperature distribution in the unit circle is determined and the Schwarz-Christoffel conformal mapping (Driscoll and Trefethen, 2002) is applied to obtain the contour probabilities for star shaped polygons. Several examples are shown with different boundary conditions. The present method does not present statistical fluctuations and is much faster than conventional iterative methods, like finite differences and finite volumes, once the probability matrix is calculated for a given geometry.

2. EXODUS METHOD

To demonstrate the application of the exodus method, the potential equation in Cartesian 2D coordinates is considered:

$$\frac{\partial^2 T}{\partial x^2} + \frac{\partial^2 T}{\partial y^2} = 0 \tag{1}$$

Making a discretization by centered finite differences with $\Delta x = \Delta y = \Delta$, it yields:

$$T_{i,j} = \frac{1}{4}(T(i+1,j) + T(i-1,j) + T(i,j+1) + T(i,j-1)) \tag{2}$$

In the classical random walk Monte Carlo method a particle is initially located in an arbitrary mesh point. For a uniform Cartesian mesh and constant properties, based on Eq. (2), the particle moves randomly to north, south, east and west directions with probability 1/4 for each direction, until reaching a boundary point where the particle accumulates the boundary value. In the standard exodus method, a modification of the classical random walk Monte Carlo method, a very large number of particles is released from a given point in the mesh. In the bidimensional Cartesian case 4 parcels are generated, each one with 1/4 of the particles moving in each direction (north, south, east, west), then the parcels reach the body boundary and accumulate the value attributed by the boundary condition.

2.1 Application of the Exodus Method to a Square Plate

An example for displacement of particles using the exodus method is shown in Figure 1 for a square plate. Rectangular plates of sides L_1 and L_2 can be easily calculated considering non-dimensional variables, $x´= x/L_1$ e $y´= y/L_2$.

Particles are released at inner points of the mesh represented by matrix $M(4\times4)$ that indicates the number of particles in the inner points and boundary points after each displacement. In Figure 1a, a large quantity of particles, for example, 1 million or more particles, or the highest number that can be stored by a computer, is placed at the point (2,2). In Figure 1b, after the first displacement, 1/4 of these particles arrives and is stored in point (1,2), 1/4 arrives and is stored in point (2,1), which are points of the plate boundary. There remains 1/4 of them in (2,3) and 1/4 of them in (3,2), that continue to move equaly distributed in each of the 4 neighbor points, as depicted in figures 1c, 1d, 1e, 1f and 1g and so on, until all particles are accumulated in the boundary points of the plate, what could take a very large computational time. To avoid this, it can be specified a maximum number of displacements or it can be specified a fraction of particles to reach the plate boundary, for example, 99 %, 99.9 % or 99.99 %. It should be noted that a particle never reaches the plate corners.

However, in the case of the matrix $M(4\times4)$ considered, the fraction of particles reaching each boundary point can be easily calculated with full precision. Let the plate boundary points be A=(1,2); B=(1,3); C=(2,4); D=(3,4); E=(4,3), F=(4,2), G=(3,3), H=(1,2), as showed in Figure 2a. The quantities of particles reaching these points are given by:

$$P_A = P_H = \frac{1}{4} + \frac{1}{32} + \frac{1}{128} + \frac{1}{512} + ... = \frac{7}{24} \tag{3}$$

$$P_B = P_C = P_F = P_G = \frac{1}{16} + \frac{1}{64} + \frac{1}{256} + ... = \frac{1}{12} \tag{4}$$

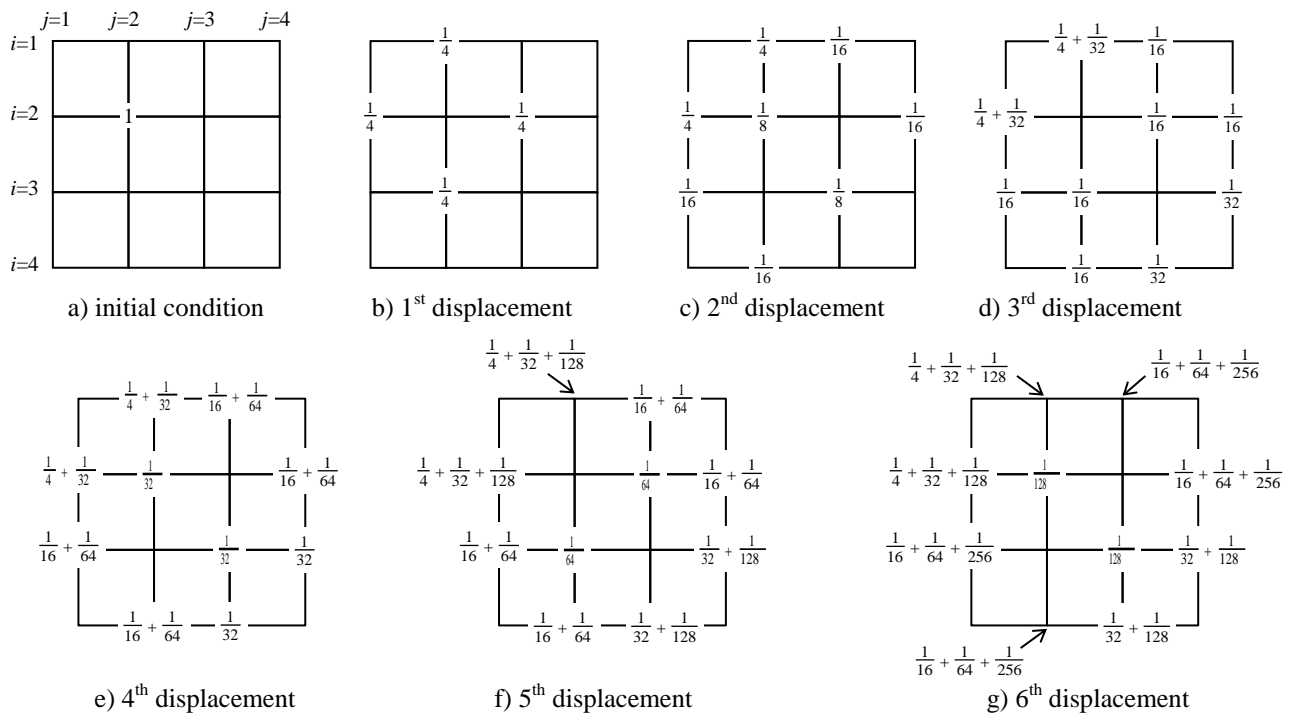$$P_D = P_E = \frac{1}{32} + \frac{1}{128} + \frac{1}{512} + ... = \frac{1}{24} \tag{5}$$

a) initial condition   b) 1st displacement   c) 2nd displacement   d) 3rd displacement

e) 4th displacement   f) 5th displacement   g) 6th displacement

Figure 1. Displacements of a large group of particles (1 trillion) leaving point (2,2).

a) boundary points   b) point (2,2)   c) point (2,3)
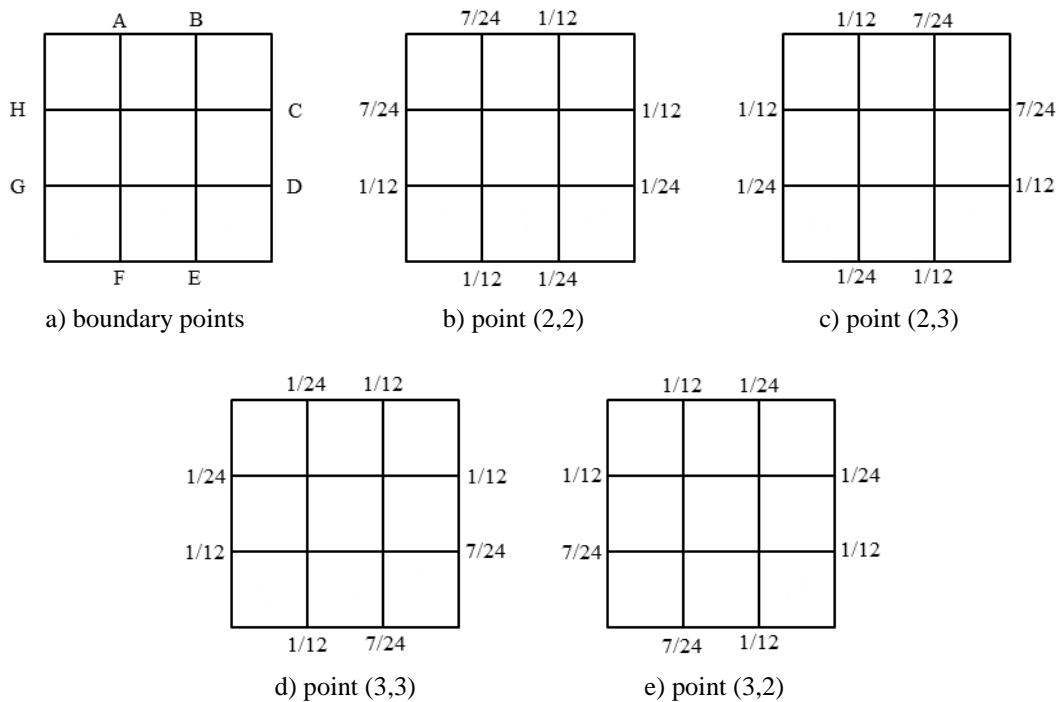

d) point (3,3)   e) point (3,2)

Figure 2. Probabilities of particles released at inner point (*i,j*) to reach the square plate boundary.

The quantities $P_{k=A,B,C,...H}$ obtained observing the sequence of values in Figure 1 also represent the probabilities of particles departing from point (2,2) to reach the boundary points. They were easily calculated because they represent the sum of terms of geometric progressions with ratio 1/4. Figure 2b shows the probabilities obtained for particles departing from point (2,2).

Due to the problem symmetry, the probabilities of particles departing from the other inner points to reach the plate boundary are equal to the probabilities for the particles leaving point (2,2), making 90° rotations, as showed in Figures 2c,d,e for points (2,3), (3,3) e (3,2), respectively. Table 1 presents the probability matrices for 4×4 and 5×5 meshes.

Once calculated the probabilities of particles leaving inner points (*i,j*) to reach the boundary points, the plate temperatures at each inner point can be determined by:

$$T(i,j) = \sum_{k=1}^{N_b} P_k(i,j)T_k \tag{6}$$

where $P_k(i,j)$ is the probability of particles leaving the mesh point (*i,j*) to reach the *k* point along the plate boundary, with temperature T_k specified, in the case of a Dirichlet problem, and N_b is the number of boundary points. In the given model, $N_b = 8$ and $k = 1, 2, ..., 8$ corresponding to points *A*, *B*, *C*, ..., *H*, respectively.

Table 1 - Probability matrices.

Mesh 4×4

Origin	k = 1	k = 2	k = 3	k = 4	k = 5	k = 6	k = 7	k = 8
(2,2)	7/24	1/12	1/12	1/24	1/24	1/12	1/12	7/24

Mesh 5×5

Origin	k = 1	k = 2	k = 3	k = 4	k = 5	k = 6	k = 7	k = 8	k = 9	k = 10	k = 11	k = 12
(2,2)	67/224	11/112	1/32	1/32	3/112	3/224	3/224	3/112	1/32	1/32	11/112	67/224
(2,3)	11/112	37/112	11/112	11/112	1/16	3/112	3/112	5/112	3/112	3/112	1/16	11/112
(3,2)	11/112	1/16	3/112	3/112	5/112	3/112	3/112	1/16	11/112	11/112	37/112	11/112
(3,3)	1/16	1/8	1/16	1/16	1/8	1/16	1/16	1/8	1/16	1/16	1/8	1/16

2.2 Temperatures in a Square Plate

A square plate with known boundary temperatures is shown in Figure 3a. Considering a 4×4 mesh and the probability values in Figure 2, or data listed on Table 1, since $T_{A,B}= 1$ and $T_{C,D,E,F,G,H} =0$, it follows that:

$$T(2,2) = P_A(2,2)T_A + P_B(2,2)T_B = 7/24 \times 10 + 1/12 \times 10 = 3.75$$

$$T(2,3) = P_A(2,3)T_A + P_B(2,3)T_B = 1/12 \times 10 + 7/24 \times 10 = 3.75$$

$$T(3,2) = P_A(3,2)T_A + P_B(3,2)T_B = 1/12 \times 10 + 1/24 \times 10 = 1.25$$

$$T(3,3) = P_A(3,3)T_A + P_B(3,3)T_B = 1/24 \times 10 + 1/12 \times 10 = 1.25$$

Figure 3c shows the calculated temperature distribution in the plate for the 4×4 mesh.

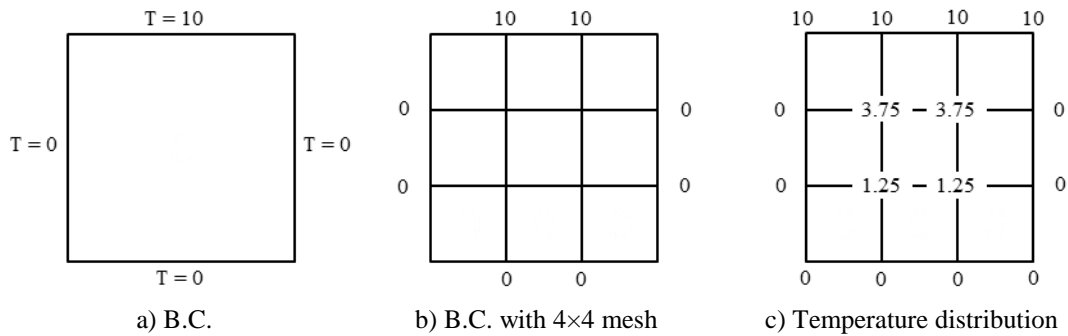a) B.C. b) B.C. with 4×4 mesh c) Temperature distribution

Figure 3 – Boundary conditions (B.C.) for a square plate and temperature distribution for a 4×4 mesh.

A computer code was written to generate probability matrices for an arbitrary $N \times N$ mesh. Figure 4a shows the results obtained using a 64×64 mesh with the top side temperature 10 and the other sides with zero temperature. The calculated temperature distributions can be compared to the Fourier series solution:

$$T_s(x, y) = \frac{40}{\pi} \sum_{k=1}^{\infty} \frac{sin((2k -1)\pi x)sinh((2k -1)\pi y)}{(2k -1)sinh((2k -1)\pi)} \tag{7}$$

Table 2 shows the mean squared error, e_{ms}, of solutions obtained by the exodus method and the Fourier series solution, using 100 terms, on the grid points, for different percentages of particles reaching the boundary. The solution obtained by Fourier series is showed in Figure 4b. In the cases listed on Table 2, the mean squared error decreases approximately linearly with N^2 and does not vary significantly with the fraction of particles reaching the mesh boundary.
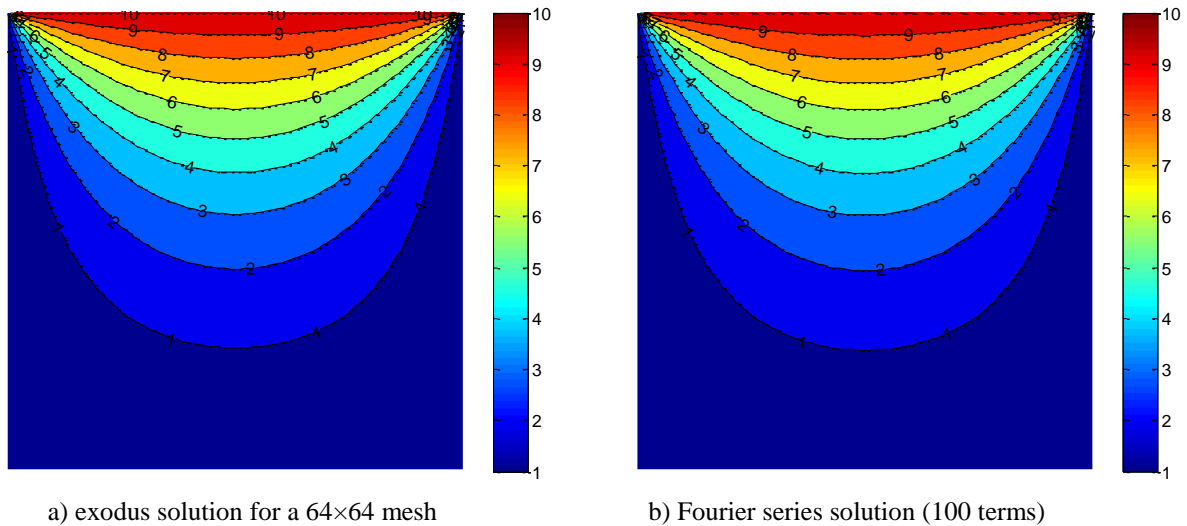

a) exodus solution for a 64×64 mesh b) Fourier series solution (100 terms)

Figure 4 – Temperature distribution in square plate heated on the top side.

$$e_{ms} = \frac{1}{N^2} \sum_{i=}^{N^2} (T - T_s)^2 \tag{8}$$

Table 2 – Mean squared error of solutions by the exodus method.

Mesh	Fraction of particles reaching the boundary		
	99 %	99.9 %	99.99 %
8×8	0.650387	0.650385	0.650385
16×16	0.312559	0.312563	0.312563
32×32	0.151546	0.151554	0.151554

2.3 Convective boundary condition

A convective boundary condition, i.e., Neumann condition, in a square plate of side L, is given by:

$$-k \frac{\partial T}{\partial x}\bigg|_{x=L/2} = h(T - T_a) \tag{9}$$

where h is the convection coefficient and T_a is the ambient temperature. After discretization, it yields:

$$T(i,N) = \frac{1}{1+h\Delta/k} T(i,N-1) + \frac{h\Delta/k}{1+h\Delta/k} T_a = \frac{N-1}{N-1+hL/k} T(i,N-1) + \frac{hL/k}{N-1+hL/k} T_a \tag{10}$$

Therefore, a new column ($N+1$) is added to the mesh with boundary condition T_a. Then, a particle in point (i,N) has the probability $(h\Delta/k)/[1+(h\Delta/k)]$ to move to ($i,N+1$) and probability $1/[1+(h\Delta/k)]$ to go back to ($i,N-1$). If a particle reaches point ($i,N+1$) it remains there and "gets" the temperature T_a, corresponding to a Dirichlet condition. For $h = 0$ a particle goes back from (i,N) to ($i,N-1$) and the particle is reflected by the boundary, corresponding to a thermal insulation. If hL/k is large, the boundary temperature becomes equal to the ambient temperature, indicating a very intense heat convection exchange with the environment.

2.4 Heat conduction in a disc

The probability matrix of a square plate can have large dimensions when the standard exodus method is applied. On the other hand, the exodus solution inside a disc requires only the calculation and the storage of a probability vector along a fixed radius in a given angle. The solution for any other angle is obtained by rotation of the calculated probability vector. Therefore, this section presents the exodus method solution for a disc. The Laplace equation in polar coordinates is given by

$$\frac{\partial}{\partial r}\left(r \frac{\partial T}{\partial r}\right) + \frac{1}{r} \frac{\partial^2 T}{\partial \theta^2} = 0 \tag{11}$$

A finite difference discretization with variable spacing is given by

$$T_{i,j} = p_{i+1,j} T_{i+1,j} + p_{i-1,j} T_{i-1,j} + p_{i,j+1} T_{i,j+1} + p_{i,j-1} T_{i,j-1}, \quad i=1,\ldots,NR, \ j=1,\ldots,NA \tag{12}$$

with $p_{i+1,j} = \frac{1}{\gamma}\left(\frac{r_i}{\Delta r_i} + \frac{1}{2}\right)$, $p_{i-1,j} = \frac{1}{\gamma}\left(\frac{r_i}{\Delta r_{i-1}} - \frac{1}{2}\right)$, $p_{i,j+1} = \frac{1}{\gamma}\frac{c}{\Delta \theta_j}$, $p_{i,j-1} = \frac{1}{\gamma}\frac{c}{\Delta \theta_{j-1}}$, $c = \frac{\Delta r_i + \Delta r_{i-1}}{r_i(\Delta \theta_j + \Delta \theta_{j-1})}$ and

$$\gamma = \frac{r_i}{\Delta r_i} + \frac{r_i}{\Delta r_{i-1}} + \frac{c}{\Delta \theta_j} + \frac{c}{\Delta \theta_{j-1}}. \tag{13}$$

where $\Delta r_i = r_{i+1} - r_i$, $\Delta r_i = r_i - r_{i-1}$, NR is the number of radii, NA is the number of angles, and $p_{m,n}$ represents the probability of a particle in the (i, j) location move to a neighbor point (m, n) in the polar grid. In the origin it can be shown that $T_1 = \frac{1}{NA} \sum_{j=1,NR} T_{2,j}$.

Figure 5 shows a polar grid with uniform spacing having $(NR, NA) = (6, 8)$. Figure 6 shows 3D plots of the probability matrices for $(NR, NA) = (20, 24)$ and $(40, 120)$. A strong decay is observed from adjacent boundary points towards inner points.

Solutions for the Laplace problem in a disc using a uniform grid with $(NR, NA) = (20, 90)$ are depicted in Figure 7, for boundary conditions $\sin(3\theta)$ and $H(x–0.1) –H(x–0.2) + H(x–0.6) – H(x–0.7)$, where H is the Heaviside step function, $x = [0, 1]$ and $\theta = [0, 2\pi]$.

The probability matrices generated for solution of the disc problem can now be directly applied to determine the full solutions in any polygonal domain using appropriate conformal mappings in the complex plane.
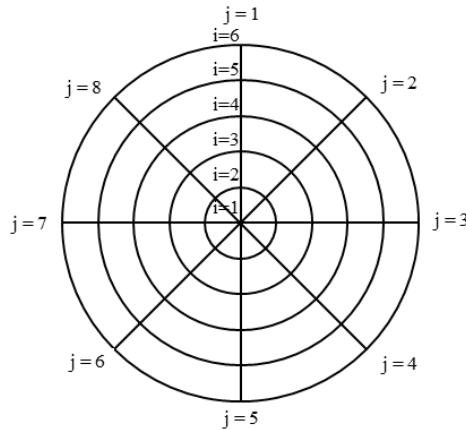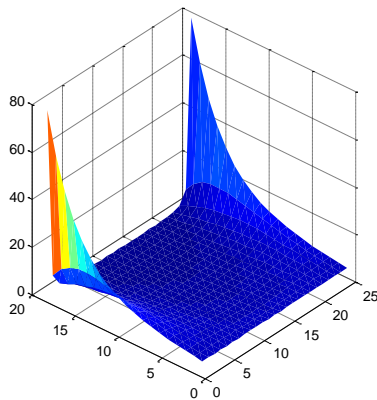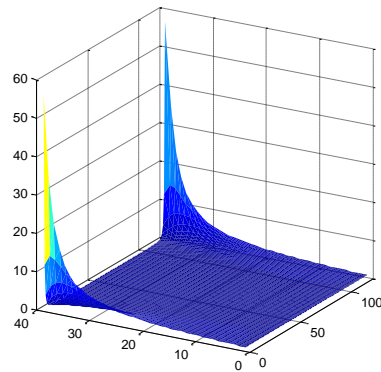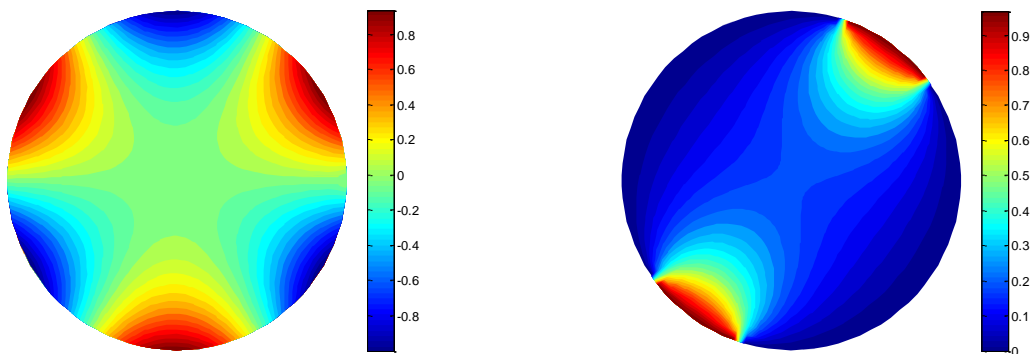

Figure 5 - Polar grid for solving Laplace equation.

a) $NR = 20$; $NA = 24$ b) $NR = 40$; $NA = 120$

Figure 6 – 3D Plots of probability matrices for different meshes.

a) $T_b = \sin(3\theta)$. b) $T_b = H(x–0.1) –H(x–0.2) + H(x–0.6) – H(x–0.7)$

Figure 7 - Exodus solution for the Laplace problem in a disc with $(NR, NA) = (20, 90)$.

2.5 Schwarz-Christoffel Transformation

A conformal mapping of the unit circle $D = \{z : |z| < 1\}$ onto an arbitrary polygonal domain is obtained by the Schwarz-Christoffel (SC) formula (Driscoll and Trefethen, 2002):

$$f(z) = C_1 \int_0^z \frac{1}{(w - \zeta_1)^{\beta_1} (w - \zeta_2)^{\beta_2} \dots (w - \zeta_N)^{\beta_N}} dw + C_2, \; z \in D \tag{14}$$

where N is the number of vertices, $\beta_i \pi (i = 1, \dots, N)$ is the exterior angle of the ith vertice of the polygon, $\zeta_i (i = 1, \dots, N)$ are the pre-images of the vertices in the unit circle, and C_1 and C_2 are scaling and rotation constants.

In the case of a m-pointed star with external angles $\beta_1 \pi$ and $\beta_2 \pi$, with $\beta_1 + \beta_2 = 2/m$, the Schwarz-Christoffel mapping is

$$f(z) = \int_0^z \frac{(1 - w^m)^{-\beta_2}}{(1 + w^m)^{\beta_1}} dw = z F_1 \left(\frac{1}{m}; \beta_1, \beta_2, \frac{m+1}{m}; z^m, z^{-m} \right) \tag{15}$$

where F_1 is the Appell F_1 function given by the series power

$$F_1(a; b_1, b_2; c; x, y) = \sum_{n=0}^{\infty} \sum_{m=0}^{\infty} \frac{(a)_{n+m} (b_1)_m (b_2)_n}{m! \, n! \, (c)_{n+m}} x^m y^n \tag{16}$$

with a, b_1, b_2 and $c \in C$, and $(x)_k = x(x+1)\dots(x+k-1)$ is the *Pochhammer* symbol. Alternatively, the Appell F_1 function can be given by the integral representation

$$F_1(a; b_1, b_2; c; x, y) = \frac{\Gamma(c)}{\Gamma(a)\Gamma(c-a)} \int_0^1 u^{a-1} (1-u)^{c-a-1} (1-ux)^{-b_1} (1-uy)^{-b_2} du \tag{17}$$

Figure 10 depicts the conformal mappings of a unit circle on m-pointed stars using Eq. (15) with a uniform grid spacing. It is seen that near the stars' vertices the resolution is low. Therefore radii close to unity need to be considered.

Figure 11 shows the distributions of temperatures inside different m-pointed stars with various boundary conditions. The unit circle was divided in 360 uniformly spaced angles and 44 non-uniformly spaced radii: $r = 0, 0.04, 0.08, \dots$ 0.36, 0.40, 0.42, 0.44, …0.96, 0.98, 0.99, 0.995, 0.999.
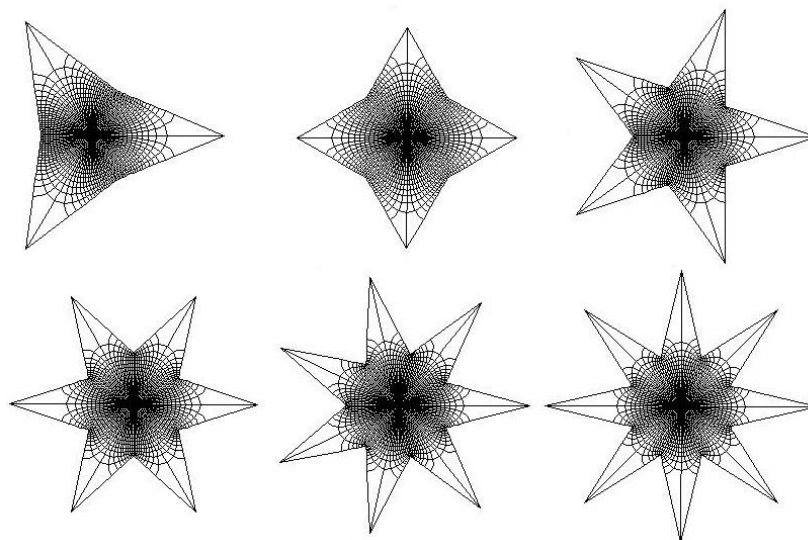

Figure 10 – *SC* conformal mappings of the unit circle on *m*-pointed stars.

a) B.C.: sin(7π*x*)   *b*) B.C.: BesselJ(1,sin(5π*x*))   *c*) B.C.: BesselJ(0,sin(π*x*))

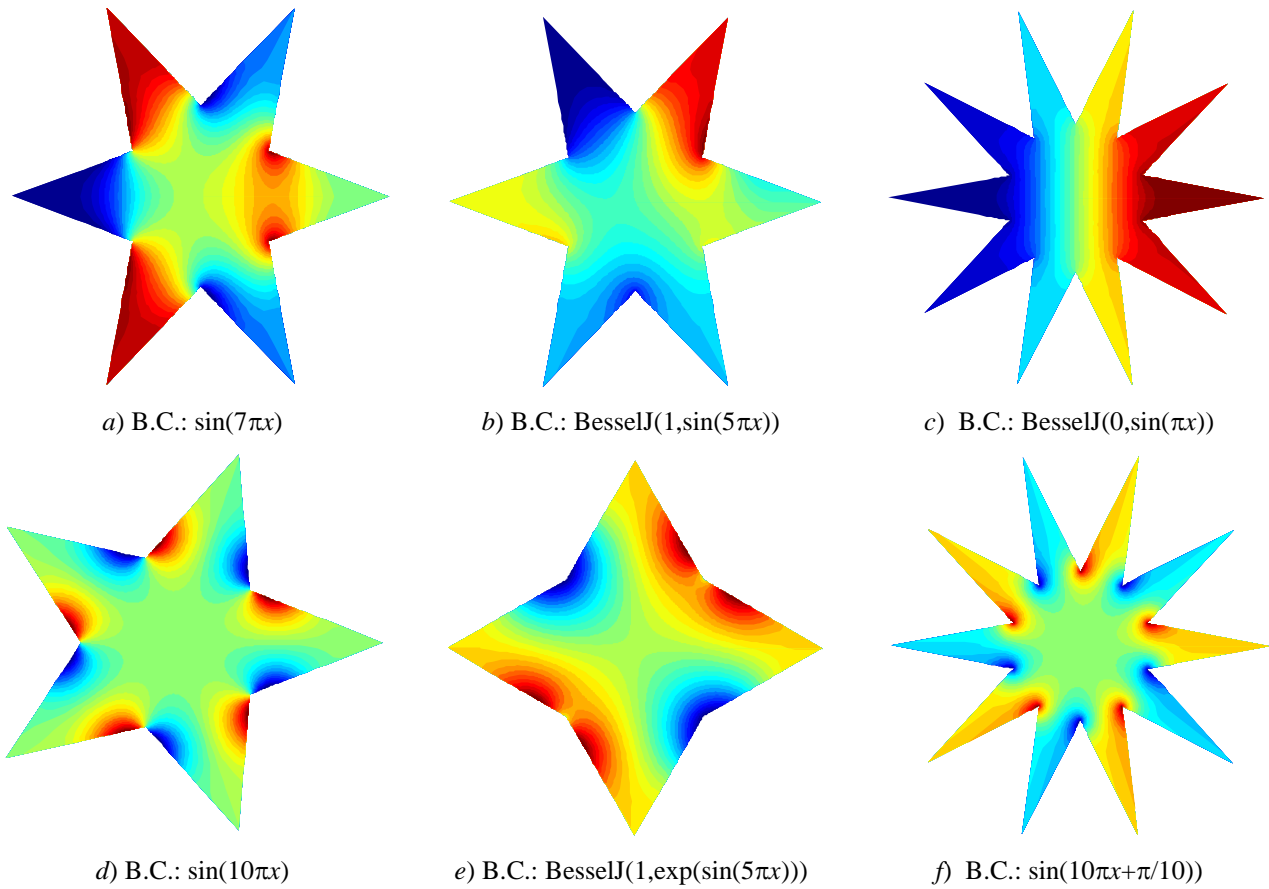*d*) B.C.: sin(10π*x*)   *e*) B.C.: BesselJ(1,exp(sin(5π*x*)))   *f*) B.C.: sin(10π*x*+π/10)

Figure 11. Temperature distributions in *m*-pointed stars using *EM* and *SC* formula for a 44 × 360 mesh and different boundary conditions (B.C.'s) along the star circumference.

3. CONCLUSION

This paper described the application of the standard exodus method, a Monte Carlo method variation, to solve rapidly heat conduction problems in star shaped objects. Initially, probability matrices were calculated and stored to determine the temperature distributions in squares and circles. Then, the Schwarz-Christoffel transformation on the unit circle was used to obtain the contour probabilities and to solve Dirichlet problems on *m*-pointed star polygons with different boundary conditions. The present method does not present statistical fluctuations and can be easily applied to any simply connected polygonal geometry using appropriate conformal mappings.

4. REFERENCES

Driscoll, T.A., Trefethen, L.N., 2002. *Schwarz-Christoffel Mapping*, Cambridge University Press, Cambridge.

Emery, A.F., Carson, W.W., 1968. A Modification to the Monte Carlo Method: The Exodus Method, *J. Heat Transfer* 90(3), pp 328-332.

Fraley, S.K., Stevens P.N., Hoffman, T.J., 1980. A Monte Carlo Method of Solving Heat Conduction Problems, *J. Heat Transfer* 102(1), pp 121-125.

Haji-Sheikh, A., Sparrow, E.M., 1967. The Solution of Heat Conduction Problems by Probability Methods, ASME *J. of Heat Transfer*, Vol. 89, p.121.

Momoh, O.D., Sadiku, M.N.O., Akujuobi, C.M., 2010. Solution of Axisymmetric Potential Problem in Spherical Coordinates Using Exodus Method, *Progress In Electromagnetics Research Symposium Proceedings*, pp. 1110-1114, Cambridge, USA.

Naraghi, M. H. N., Tsai, S.C., 1993. *Numerical Heat Transfer, Part B: Fundamentals*, Vol. 24, No. 4, pages 475-487.

5. RESPONSIBILITY NOTICE

The author is the only responsible for the printed material included in this paper.